

Repair Maintenance of Diesel Engine Cylinder Head

M. A. Morsy^{*1} and E. El-Kashif²

Central Metallurgical R&D Institute, Cairo, Egypt¹,
Metallurgy Dept., Faculty of Engineering, Cairo University², Cairo, Egypt. [*morsy_abokhala@yahoo.com](mailto:morsy_abokhala@yahoo.com)

Abstract: This paper presents many trials to repair a diesel engine cylinder head made of pearlitic grey cast iron, which was used in a truck. The cylinder head was repaired due to the existence of cracks at the junction between the valve seat and the heater plug seat. Shielded metal arc welding (SMAW) process using different electrodes was applied. The increase in preheating temperature resulted in a formation of a continuous carbide layer in the partial fusion zone and a decrease in martensite phase formed at the heat affected zone. However, the decrease in preheat temperature resulted in an increase of martensite at the heat affected zone and a decrease in the carbide layer at the partial fusion zone. Most of the SMAW electrodes resulted in the formation of regions with high hardness values which imply that the repair welding of the cylinder head using these electrodes is inefficient. Application of the powder flame spray method in repair welding of the cylinder head resulted in partial fusion zone and heat affected zone with hardness values comparable to that of base metal. Preheating in furnace to 500 °C then immediately putting the specimen in the furnace at the same temperature for 1 hour after applying powder flame spray gave excellent hardness results for the heat affected zone (HAZ) and partial fusion zone (PFZ).

[M. A. Morsy and E. El-Kashif. Repair Maintenance of Diesel Engine Cylinder Head. Journal of American Science 2011;7(3):158-168]. (ISSN: 1545-1003). <http://www.americanscience.org>.

Keyword: Failure of cylinder head, Pearlitic gray iron, SMAW, Flame spray method, Heat affected zone, Partial fusion zone, Hardness distribution, Microstructure.

1. Introduction:

In an internal combustion engine, the cylinder head sits above the cylinders consists of a platform containing part of the combustion chamber and the location of the valves and heater plugs. In Diesel engines, the cylinder heads are usually made of grey cast iron. The cylinder head is a crucial part of all combustion engines, and its cracking can result in catastrophic damage to the engine. The most common cause of cylinder head cracking is overheating. When a vehicle overheats, it puts stress on all of its metal components, including the cylinder head, which is often at the center of the heat. Xu and Yu studied the failure on a diesel engine cylinder head made of grey cast iron. The crack was initiated from the interior wall and propagated toward the exterior surface of the cylinder head. Their results showed that longer graphite flake and more amount of ferrite are the general metallurgical characteristics of the failed cylinder head, compared with the specified, which may lead to the lower whole hardness of the material. They added that in the crack origin zone, a network of grain boundary connected flake graphite was found. The appearance of this network grain boundary flake graphite decreases the strength of this zone and initiates the crack [1].

Cast irons are among the most difficult metals to weld because they contain high carbon

content, and a wide range of microstructures. The part of the base metal that reaches a temperature high enough to cause metallurgical changes, but not high enough to cause melting is the HAZ. In this zone, the matrix is transformed to hard martensitic structure upon rapid cooling which cause brittleness. Brittleness associated with martensite which can be reduced by maintaining a high preheat during welding, followed by slow cooling, or a post weld heat treatment [2-7]. The weld metal and fusion zones are other potential problem areas, when molten cast iron is cooled rapidly; the carbon is not rejected from the melt as graphite, but forms hard brittle iron carbide which is susceptible to cracking and difficult to machine [4-7].

Thermally sprayed nickel-based alloy coatings are used in a variety of applications, e.g. as bond coats for thermal barrier coatings (TBCs) on turbine components, as restorative layer for machine parts, as bond coats in internal combustion engine cylinders, for corrosion protection of boiler tubes and in other numerous applications requiring wear, high temperature and corrosion resistant surfaces [8-13]. Repair maintenance of pearlitic gray-cast iron cylinder head using thermal spray technique should be systematically studied in order to give better insight into the capability of this technique.

In this study shielded metal arc welding (SMAW) with different electrode types were used to repair a pearlitic gray cast iron and the results were compared with that obtained by using thermally sprayed nickel-based alloy powder.

2. Experimental work

2.1 Material

2.1.1 Cylinder head

In an internal combustion engine, the cylinder head sits above the cylinder and consists of a platform containing part of the combustion chamber and the location of the valves and heater plugs. The most common cause of cylinder head cracking is overheating. The cracks were detected using magnetic particle test. One of the cracks detected by fluorescent magnetic particle test is shown in Fig. 1.



Fig. 1 Crack as detected by fluorescent magnetic particle test

Chemical analysis of cylinder head material is carried out using optical emission spectrometer. The composition of the cylinder head material is shown in Table 1.

Table 1 Chemical composition of cylinder head, mass%

Element	C	Si	Mn	P	S	Cr	Mo	Ni	Fe
mass %	3.76	1.94	0.669	0.0321	0.0218	0.165	0.37	0.283	balance

2.1.2 Repair welding materials

Different types of Shielded Metal Arc Welding (SMAW) electrodes are applied in this

work. Table 2 shows the different electrodes used and the chemical composition of their weld metals.

Table 2 Chemical composition of weld metal for different electrodes, mass%

Electrode	Element									
	C	Mn	Si	P	S	Cu	Ti	Al	Ni	Fe
JIS DFC Fe	0.15	0.8	1	0.03	0.04	–	–	–	–	Balance
AWS A5.11 E Ni –Cu-7	0.04	3	0.7	0.01	0.001	29	0.7	0.3	Balance	1
AWS A5.15 E Ni-Fe-CI	0.5	–	–	0.2	0.001	–	–	–	53	Balance

Also, a thermal spray powder is applied for the repair welding process; its chemical composition is shown in Table 3. The average particle size of the

powder is -53 to +20 μm ; the hardness of the powder is in the range 190-260 HV.

Table 3 Chemical composition of flame spray powder, mass%

Element	C	Fe	B	Si	Ni
mass%	0.03	0.5	1.4	2.4	Balance

2.2 Repair Welding Procedure

2.2.1 Test specimens

To examine the best technique for repair of the pearlitic grey cast iron cylinder head, test specimens with a groove angle of 90° and a groove depth of 15 mm was prepared from the cylinder head.

2.2.2 Welding conditions

Three different electrodes were applied in SMAW process. The welding conditions are shown in Table 4.

Peening is applied after each pass to remove residual stresses and oxide layers formed. After welding, all specimens were allowed to cool slowly in sand.

2.2.3 Repair welding using thermal spray powder

Powder flame spraying process was also applied in repair welding of cylinder head. Preheating temperatures of 500°C is applied before thermal spray application followed by cleaning of the groove faces by grinding and brushing.

Thermal spraying process was applied using two different post weld heating cycles. In the first one, the specimen after thermal spray was left to cool to room temperature in sand. In the other, the specimen was held for 1 hour at 500°C in a Muffle furnace then furnace cooled to room temperature.

Table 4. Welding conditions for different SMAW electrodes

Electrodes	Voltage, V	Current, A	Electrode size, mm	Preheating Temperature, °C	Polarity
AWS A5.15 E NiFe-CI	24	100	3.2	100 and 400	DCEP
JIS Z3252 DFC Fe	24	100	3.2	100	DCEP
AWS A5.11 E NiCu-7	24	100	3.2	100	DCEP

2.3 Microstructure Observation

Microscopic examination is conducted at the cross section specimens. The specimens were cutout using fine cutter with cooling. The cross section was then ground through grit Silicon papers (180 to 1000). Final polishing was performed using 0.5 µm alumina paste, then cleaned and dried. The polished specimens are etched by 2% Nital solution to reveal the cast iron structure. Etching solution of 50 % Nitric acid, 50% Acetic acid are used to reveal the weld microstructures of AWS E NiFe-CI and AWS E NiCu-7 welds. Microstructure of base metal and welded specimens were observed using optical microscope.

2.4 Micro-hardness Measurements

Micro-hardness was conducted using Shimadzu Vicker micro-hardness testing device with a load of 9.807 N and 15 sec loading time.

3. Results and Discussion

3.1 Cylinder head Properties

The microstructure of the base metal is shown in Fig. 2. The microstructure shows gray cast iron that contains flakes of graphite in a pearlitic matrix. The average value of the base metal hardness is 215 HV.

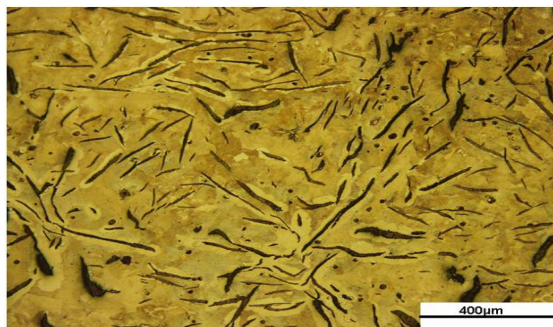


Fig.2 Microstructure of base metal cylinder head

The weldability of cast iron is very low. Thus, optimizing the welding conditions such as preheating and PWHT can improve the properties of the weldment. Three arc welding electrodes were selected to repair the cylinder head using different conditions. The results will be discussed based on the microstructures of weldments and their hardness distribution along weld metal, partial fusion zone, and heat affected zone.

For the sake of comparison, Powder flame spraying process was also applied in repair welding of cylinder head.

3.2 Repair of Cylinder head Using Carbon Steel Electrode

Cast iron was welded under welding conditions mentioned in Table 4 using JIS Z3252 covered electrode - DFCFe with preheating temperature of 100°C.

3.2.1 Microstructure

Microstructures of the cross section after welding using carbon steel electrode are shown in Figs. 3-5. Figure 3 shows the microstructure of weld metal, partial fusion zone, and heat affected zone. The weld metal near the fusion zone is in a dendritic form. The partial fusion zone contains some carbides which are not continuous as shown in Fig.3. The heat affected zone shows the existence of some martensite as shown in Fig. 4. Weld metal shows the existence of carbides and martensite as shown in Fig.5.

3.2.2 Micro-hardness distribution

Figure 6 shows micro-hardness distribution of weld metal, PFZ and HAZ. The micro-hardness value of the carbides in the PFZ is very high compared with that of the base metal.

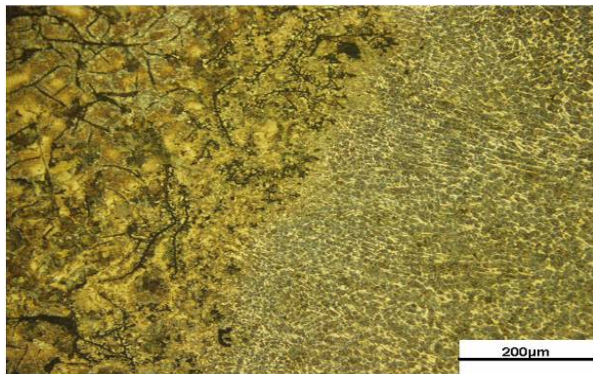


Fig. 3 Microstructure of weld metal, PFZ and HAZ of the specimen welded using carbon steel electrode

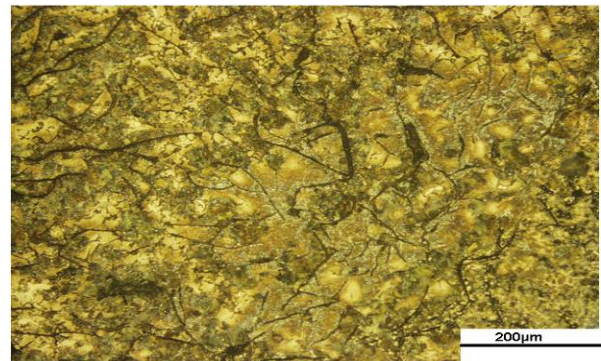


Fig. 4 Microstructure of the HAZ of the specimen welded using carbon steel electrode.

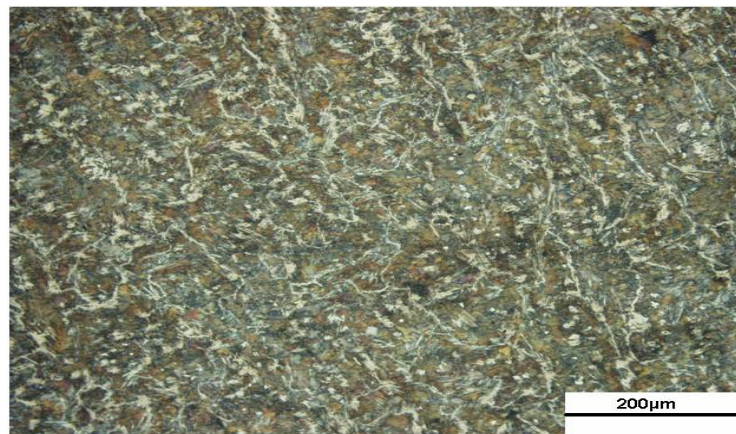


Fig. 5 Microstructure of the weld metal of the specimen welded using carbon steel electrode.

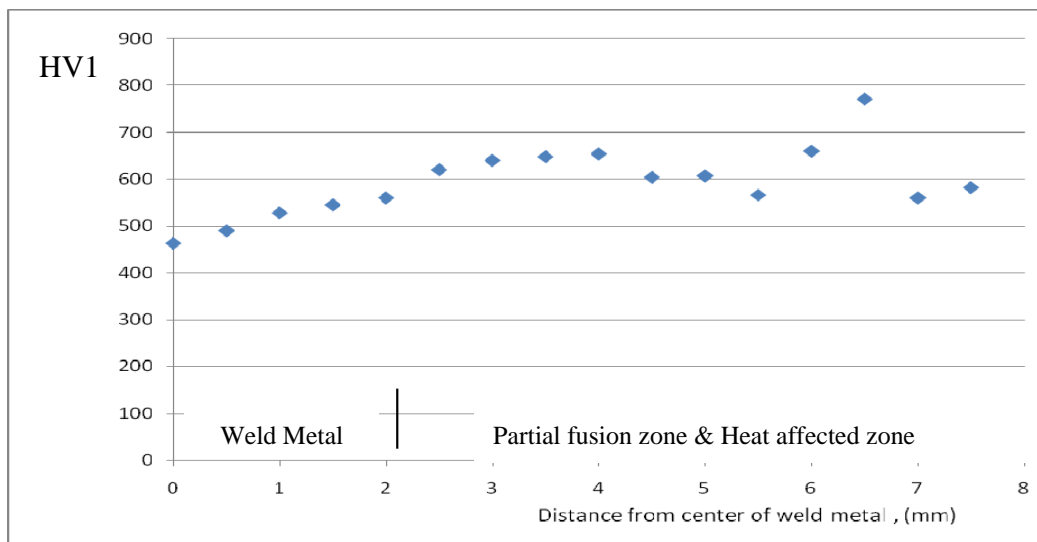


Fig. 6 Micro-hardness distribution using carbon steel electrode

3.3 Repair of Cylinder Head Using Nickel-Copper Electrode

Cast iron was welded under welding conditions mentioned in Table 4 using AWS A5.11 – E Ni Cu-7 electrode. Its chemical composition is shown in Table 2 and the preheat temperature was 100°C.

3.3.1 Microstructure

Microstructures of the cross section after welding are shown in Figs. 7-9. PFZ shows the existence of carbides as shown in Fig. 7. Microstructure of weld metal shows the dendritic structure of austenitic structure of Copper-Nickel alloy as shown in Fig. 8. The HAZ microstructure shows the existence of some martensite and a network of grain boundary connected flake graphite as shown in Fig.9.

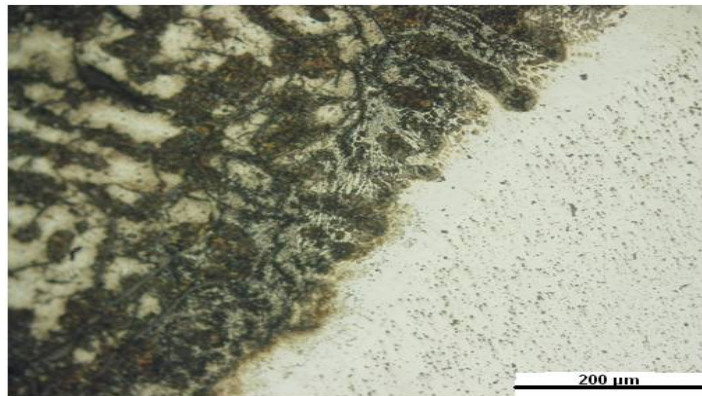


Fig. 7 Microstructure of weld metal, PFZ and HAZ using Nickel - Copper alloy electrode

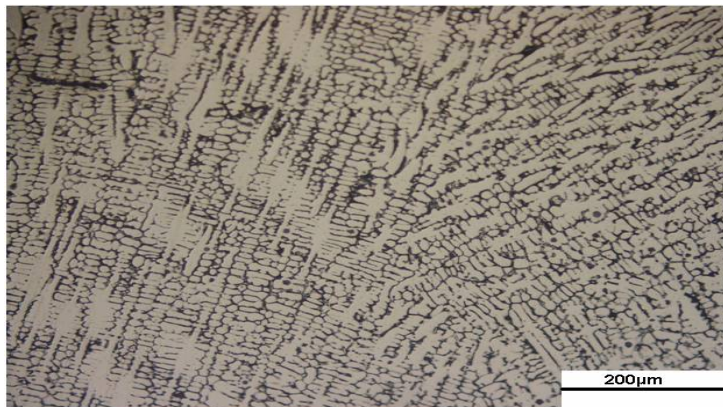


Fig. 8 Microstructure of weld metal using Nickel- Copper alloy electrode

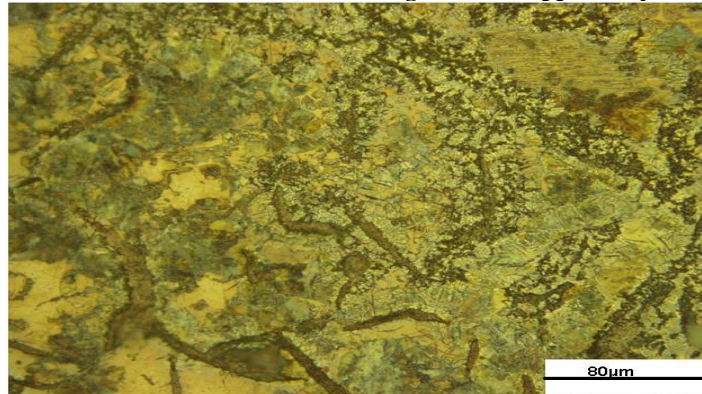


Fig. 9 Microstructure of HAZ using Nickel-Copper alloy electrode

3.3.2 Micro-hardness distribution

Figure 10 shows micro-hardness distribution of weld metal, PFZ and HAZ using Ni-Cu electrode. The micro-hardness value of the carbides in the PFZ

is as high as 754 HV which is very high compared with that of base metal (215 HV) which acts as an area susceptible to crack initiation and propagation at the fusion line.

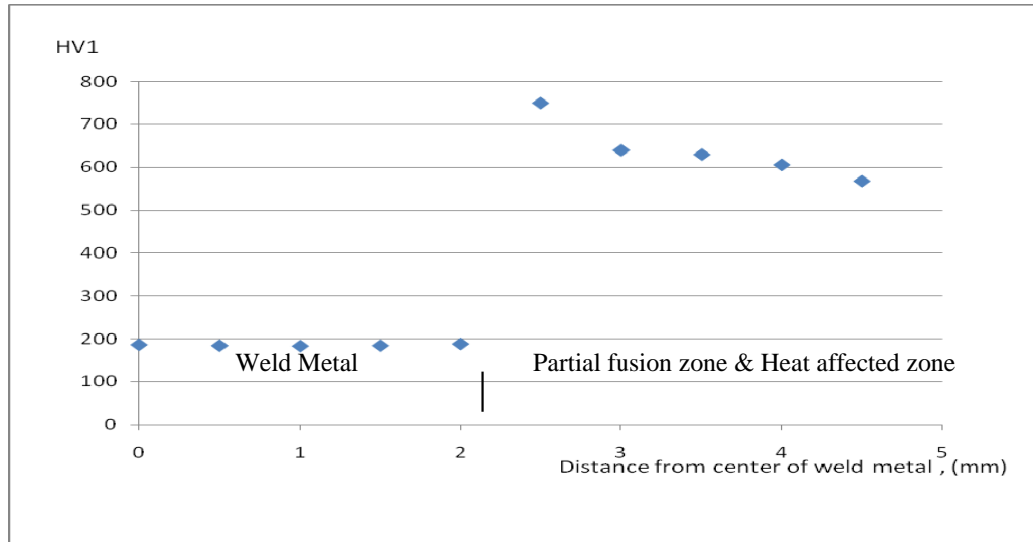


Fig. 10 Micro-hardness distribution for Nickel-Copper electrode

3.4 Repair of Cylinder Head Using AWS A5.15-E NiFe-CI

3.4.1 Using preheat temperature of 100°C

Cast iron was welded under welding conditions mentioned in Table 4 using AWS A5.15 E Ni-Fe-CI electrode. This electrode was used with a preheat temperature of 100°C.

3.4.1.1 Microstructure

Microstructures of the cross section after welding are shown in Figs. 11-13. The microstructure of the PFZ shows a few amounts of carbides which is discontinuous as shown in Fig. 11. However, Fig. 12 shows the existence of martensite at the HAZ. Figure 13 shows the dendritic structure of iron nickel alloy.

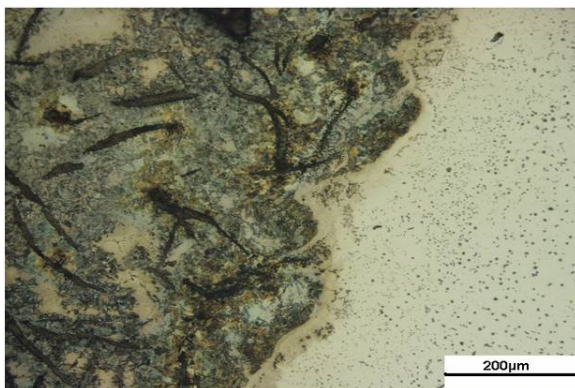


Fig. 11 Microstructure of PFZ of the specimen welded using Iron Nickel cast iron electrode; preheat temperature of 100°C.

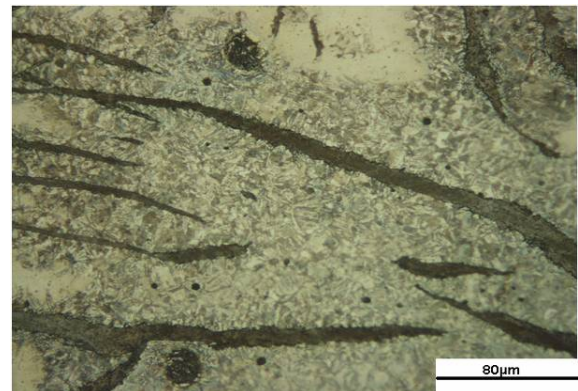


Fig. 12 Microstructure of HAZ of the specimen welded using Iron Nickel cast iron electrode; preheat temperature of 100°C.

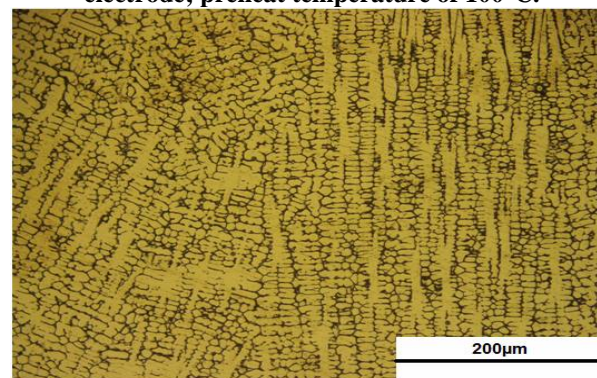


Fig. 13 Microstructure of weld metal of the specimen welded using Iron Nickel cast iron electrode; preheat temperature of 100°C.

3.4.1.2 Micro-hardness distribution

Figure 14 shows the micro-hardness distribution of the weld metal, PFZ and HAZ of the

specimen welded using ENiFe-CI electrode. Martensite formed in heat affected zone caused an increase in its hardness.

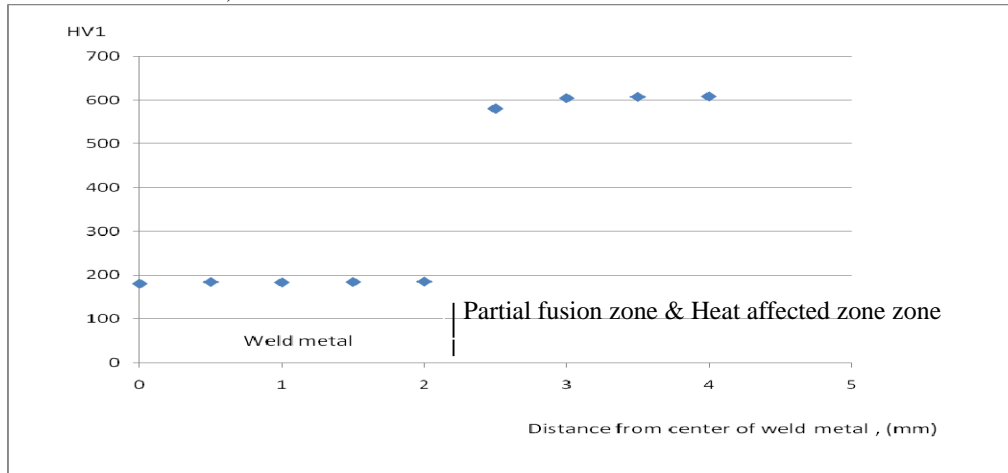


Fig. 14 Micro-hardness distribution using Ni-Fe-CI electrode and preheat temperature of 100°C.

3.4.2 Using preheat temperature of 400°C

Cast iron was welded under welding conditions mentioned in Table 4 using AWS A5.15 E NiFe-CI. This Electrode was used by applying a preheat temperature of 400°C.

3.4.2.1 Microstructure

Microstructures of the cross section after welding are shown in Figs 15 and 16. Figure 15 shows weld metal, PFZ and HAZ. There are continuous carbides in the PFZ. HAZ shows less martensite compared with the specimen preheated to 100°C as shown in Fig. 16.

Weld metal shows the dendritic structure of NiFe-CI alloy as shown in Fig. 17. Austenite grains of nickel alloy with carbides appear in Fig. 17.

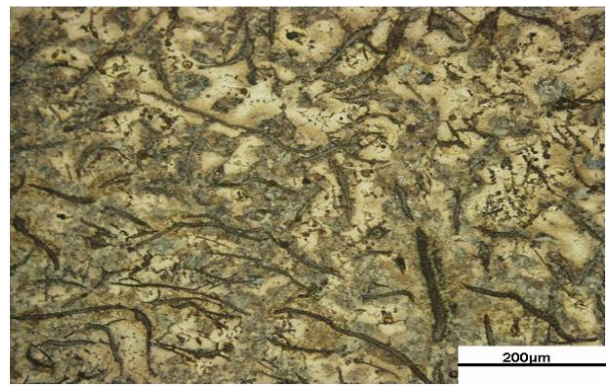


Fig. 16 Microstructure of HAZ of the specimen welded using Nickel Iron Cast Iron Electrode.

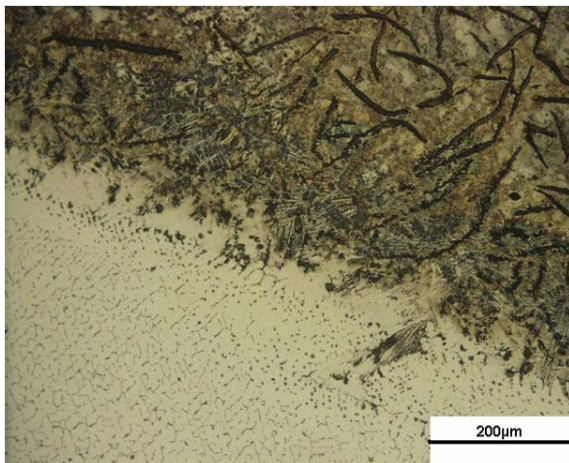


Fig. 15 Microstructure of PFZ of the specimen welded using Nickel Iron Cast Iron Electrode

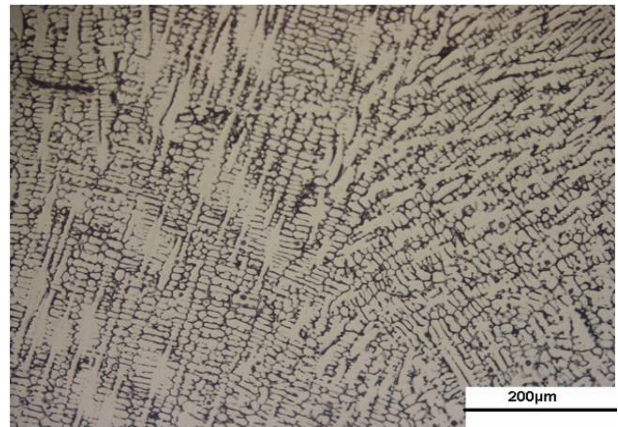


Fig. 17 Microstructure of weld metal using Iron-Nickel Iron Cast Iron Electrode.

3.4.2.2 Micro-hardness distribution

Figure 18 shows micro-hardness distribution of the specimen repaired using ENiFe-CI electrode after preheating at 400 °C.

The micro-hardness values of the partial fusion zone are much higher than weld and base metal due to presence of carbides however the heat affected zone shows lower values of hardness due to low martensite area fraction.

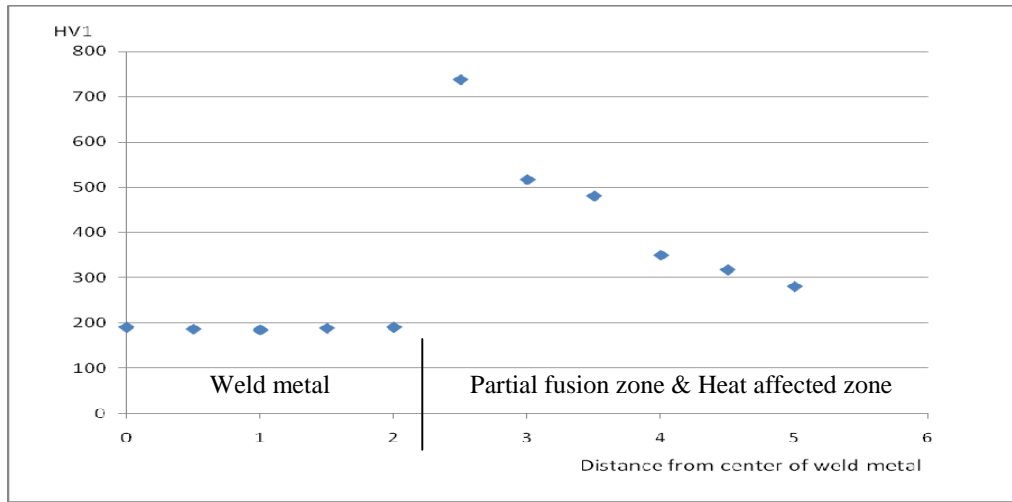


Fig. 18 Micro-hardness distribution for the specimen welded using Iron Nickel Cast Iron Electrode with preheat temperature 400°C

3.4.3 SMAW processes evaluation

The previous results using different electrodes indicated that increasing preheat temperature resulted in the formation of continuous carbides at the partial fusion zone with less martensite at heat affected zone. However low preheating temperature resulted in formation of fewer carbides at partial fusion zone and formation of large area fraction of martensite in the heat affected zone. Thus a low preheating temperature is preferred in welding of cast irons, due to the fewer amounts of carbides formed. However, it is impossible to achieve a solidification cooling rate sufficiently low to completely avoid carbide formation [15,16]. It is also possible to use low heat input as possible to minimize the formation of the PFZ, i.e., to create a steep temperature gradient which will reduce the thickness of the PFZ. In this study, the heat input was the same for all electrodes used (1.44 kJ/mm) and the Ni-Fe electrode showed the smallest PFZ (0.2mm) with a preheat temperature of 100°C. However, increasing the preheat temperature to 400°C results in larger PFZ (0.8mm) for the same electrode which is in agreement with the results obtained by Askeland and Birer obtained for tempered nodular cast iron weldments [14].

3.5 Repair Welding of Cylinder Head Using Thermal Spray Powder

Ni-base powder thermal spray is applied

using oxy-acetylene flame to weld the test specimen. The powder chemical composition was shown in Table 3.

4.5.1 Specimen A

The specimen was subjected to uniform preheating at 500°C then buried in sand to slowly cool after thermal spraying.

4.5.1.1 Microstructure

Microstructures of the cross section after welding are shown in Figs. 19- 21.

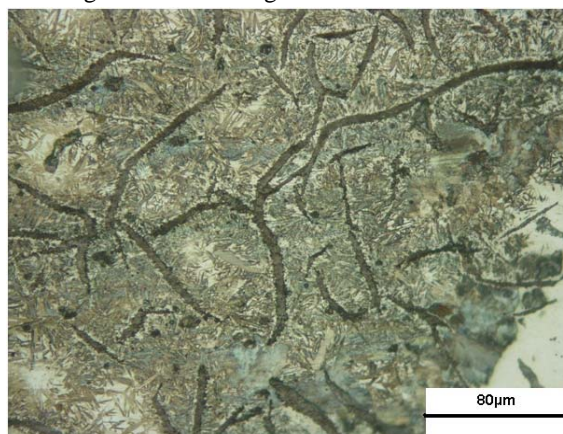


Fig. 19 Microstructure of heat affected zone of specimen A

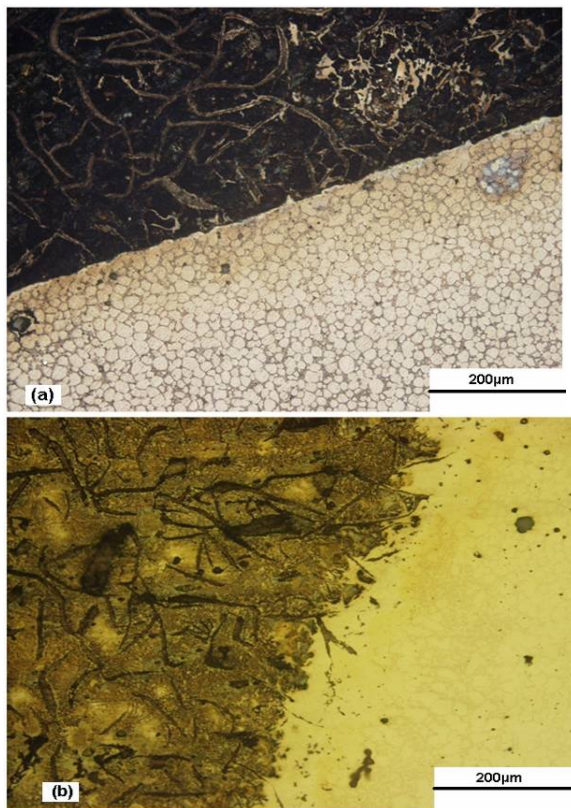


Fig. 20 Microstructure of weld metal, PFZ, and HAZ for specimen A, (a) Etching of weld metal only, (b) Etching of base metal

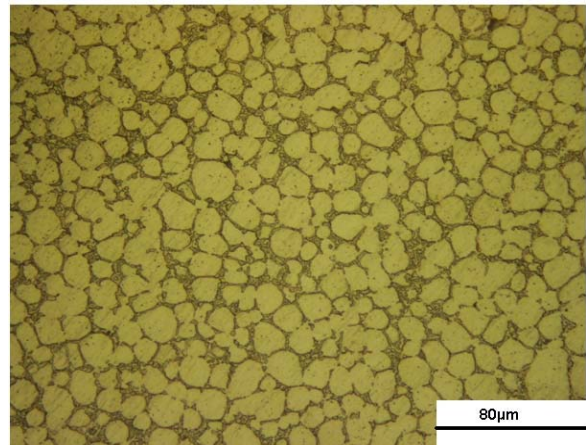


Fig. 21 Microstructure of Weld metal for specimen A

There is a doubt of the existence of partial fusion zone as shown in Fig. 20. However, HAZ shows the existence of martensite as shown in Fig. 20. Microstructures of weld metal are shown in Fig. 21 which shows the gamma phase of Nickel and the eutectic structure at grain boundaries.

3.5.1.2 Micro-hardness Distribution

Figure 22 shows micro-hardness distribution through the weld metal, PFZ and HAZ for the thermal sprayed specimen A. The presence of martensite in HAZ raised its hardness values to be in the range of 500-600 HV. This value is also higher than that of base metal.

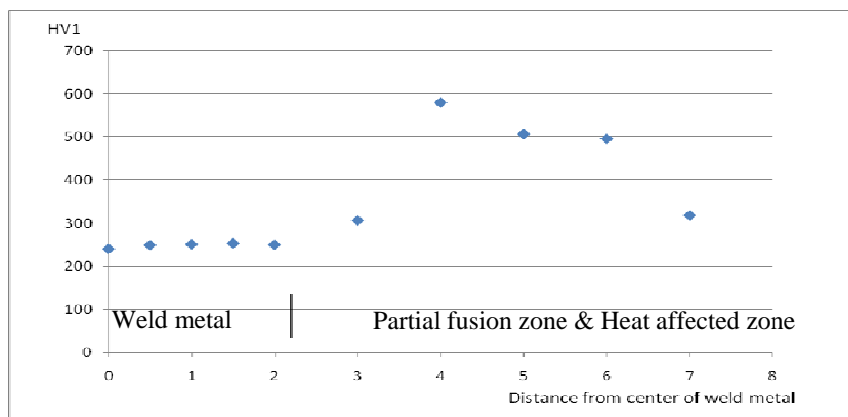


Fig. 22 Micro-hardness distribution for specimen A

3.5.2 Specimen B

The specimen was subjected to uniform preheating of 500°C; then thermally sprayed and

immediately kept at 500°C for 1 hour and allowed to cool slowly to room temperature in the furnace.

3.5.2.1 Microstructure

Microstructures of weld metal, PFZ and heat affected zone are shown in Figs 23 and 24. There is a doubt of the existence of PFZ (No carbide formation)

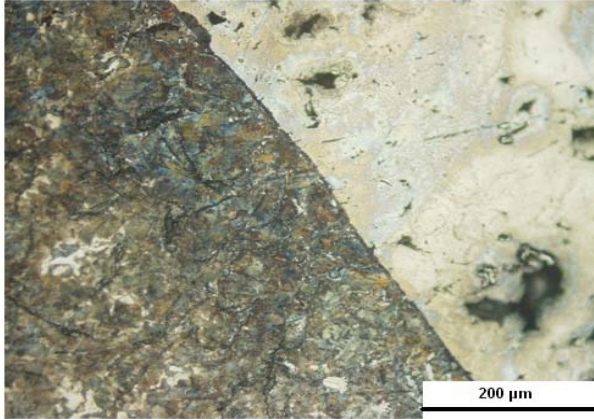


Fig. 23 Microstructure of weld metal, PFZ, and HAZ of specimen B

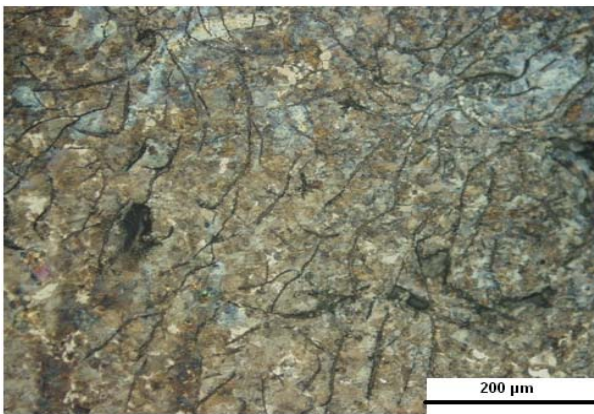


Fig. 24 Microstructure of HAZ of specimen B

and the heat affected zone is a pearlitic matrix. This achieves the two optimum conditions which are: 1. Carbides free PFZ and 2. Least martensite in the HAZ.

3.5.2.2 Micro-hardness distribution

The micro-hardness distribution of specimen B is shown in Fig. 25. The micro-hardness values of the HAZ and PFZ are close to the values of the base metal hardness. It is well known that the crack initiation and propagation in cast iron welds are due to the difference in mechanical properties between the base metal and weld metal. Using the technique followed with specimen B, such difference could be eliminated to a large extent and an average hardness of 300 HV was obtained for both PFZ and HAZ which is comparable to the hardness of the base metal (215 HV).

Some researchers [17] studied the restoration by welding of ductile cast iron and they concluded that trial and error procedure development may be necessary to get lower thickness of the martensite zone and discontinuous carbide network in addition to a pearlitic HAZ. Using thermal spray technique, the trial and error procedure which was applied in welding of cast irons may be eliminated and better welding properties were obtained.

Using of this technique, the cylinder head was repaired successfully and it is working since two years with 12 hours working time per day, which imply the reliability of this technique. Furthermore, it saves the cost of purchasing new cylinder heads for this large number of trucks.

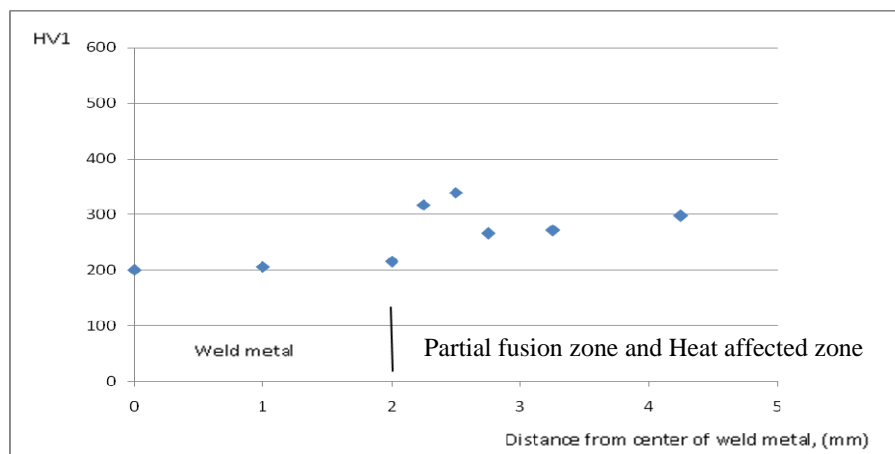


Fig. 25 Micro-hardness distribution of specimen B

4. Conclusions:

Repair welding of cylinder head was carried out primarily using shielded metal arc welding (SMAW) process with the following types of electrodes: AWS A5.15 ENiFe-CI, JIS DFC Fe (carbon steel electrode) and AWS A5.11 E Ni-Cu-7.

Welding using SMAW with AWS ENiFe-CI electrode was carried out after preheating to 100°C and 400 °C as well. High preheating temperature caused formation of continuous carbide layer in the partial fusion zone and formation of few amount of martensite in the heat affected zone. Low Preheat temperature of 100°C caused formation of a fewer amount of carbides in partial fusion zone, however higher amount of martensite was formed in the heat affected zone.

Hardness distribution of the specimens welded by SMAW using the three electrodes indicated that hardness values at partial fusion zone and heat affected zone were very high when compared with base metal hardness but the Ni-Fe electrode showed the lowest hardness values compared with the other two electrodes.

The other alternative was using powder flame spray process with preheating temperature of 500°C. Thermal spraying process was applied twice, at the first time the specimen was cooled in sand, and the other specimen was hold for 1 hour at 500 °C and slowly cooled in a muffle furnace at. The two specimens did not show formation of carbides, but the specimen cooled in sand showed formation of martensite in the heat affected zone. The other specimen that was cooled in the furnace showed a microstructure that is free of martensite and carbides, hardness distribution for this specimen showed comparable hardness values for partial fusion zone and heat affected zone with that of the base metal which imply the success of this technique to be applied in repair of pearlitic gray cast iron.

Corresponding author

M. A. Morsy
CMRDI, Cairo, Egypt
morsy_abokhala@yahoo.com

5. References:

1. X. Xu and Z.Yu, "Failure Analysis of a diesel engine cylinder head", *Engineering Failure Analysis*, Vol. 13 (2006) 1101–1107.
2. The Joining and Fabrication of Nodular Iron Casting by Welding, S.G. Iron Produces Association, London, 1970.
3. Castolin Societe Anongome, "Cast Iron" Technical Report, (1985) 1–20.
4. E. Huke and H. Udin, "Welding metallurgy of nodular cast iron", *Weld. J.*, Vol. 32, (1953) 378s–385s.
5. E. Nippes, "The heat affected zone of arc welded ductile iron", *Weld. J.*, Vol. 39, (1960) 465–472.
6. G. Pease, "The welding of ductile iron", *Weld. J.* 39, (1960) 1-9.
7. H. Megahed, "Effect of weld heat input, number of passes and interpass temperature on the mechanical and structural properties of ductile cast iron", *J. Eng. Appl. Sci., Fac. Eng., Cairo University*, Vol. 42, (1995) 931–947.
8. L. Pawlowski, "The Science and Engineering of Thermal Spray Coatings", Wiley, 1995.
9. K. Tani, Y. Harada and Y. Kobayashi, "Unusual application of plasma-sprayed coatings for boiler tubes in oil-fired boilers ", *Proceedings of Fifteenth International Thermal Spray Conference*, (1998) 951–956.
10. W. Brindley, " Thermal barrier coatings for aircraft engines: history and directions" *J. Thermal Spray Technol.* Vol. 6, No. 1 (1997) 35-42.
11. R. Unger, *Proceedings of National Thermal Spray Conference*, ASM International, Materials Park, OH, (1987) 365–370.
12. D. Cook, "Materials science and engineering", Ph.D. thesis, SUNY, Stony Brook, 2001.
13. S. Sampath, G. Bancke, H. Herman, and S. Rangaswamy , "Plasma Sprayed Ni-Al Coatings ", *Surf. Eng.*, Vol. 5 No. 4 (1989).
14. D. Askeland, and N. Birer, "Secondary graphite formation in tempered nodular cast iron weldment", *Weld. J.*, Vol. 52 (1979) 337–341.
15. R.Voight and C. Loper, "A study of heat affected zone structures in ductile cast iron", *Weld. J.*, Vol. 62 (1983) 82–88.
16. R.Voight and C. Loper, "Welding metallurgy of grey and ductile cast irons", *AFS Trans.*, Vol. 94 (1986)133–146.
17. E. El-Banna, M. Nageda, and M. Abo El-Saadat, "Study of Restoration by Welding of pearlitic ductile cast irons", *Materials letters*, Vol. 42, (2000) 311–320.

2/8/2011